Soft Matter

PAPER

View Article Online
View Journal | View Issue

Cite this: *Soft Matter*, 2014, **10**, 4609

Bile acid–surfactant interactions at the liquid crystal/aqueous interface

Sihui He,[a] Wenlang Liang,[b] Kung-Lung Cheng,[c] Jiyu Fang*[b] and Shin-Tson Wu*[a]

Received 3rd March 2014
Accepted 8th April 2014

DOI: 10.1039/c4sm00486h

www.rsc.org/softmatter

The interaction between bile acids and surfactants at interfaces plays an important role in fat digestion. In this paper, we study the competitive adsorption of cholic acid (CA) at the sodium dodecyl sulfate (SDS)-laden liquid crystal (LC)/aqueous interface formed with cyanobiphenyl (*n*CB, $n = 5–8$) and the mixture of 5CB with 4-(4-pentylcyclohexyl)benzonitrile (5PCH). We find that the critical concentration of CA required to displace SDS from the interface linearly decreases from 160 μM to 16 μM by reducing the alkyl chain length of *n*CB from $n = 8$ to $n = 5$ and from 16 μM to 1.5 μM by increasing the 5PCH concentration from 0 wt% to 19 wt% in the 5PCH–5CB binary mixture. Our results clearly demonstrate that the sensitivity of 5PCH–5CB mixtures for monitoring the interaction between CA and SDS at the LC/aqueous interface can be increased by one order of magnitude, compared to 5CB.

1. Introduction

Bile acids are important biological surfactants synthesized by the liver from the enzymatic catabolism of cholesterol.[1] Unlike some traditional surfactants, which typically have a hydrophilic head group bonded to a linear, flexible, hydrocarbon tail, bile acids have a large, rigid, quasi-planar steroid ring system with a hydrophilic α face and a hydrophobic β face. The facial amphiphilic nature and unique structure of bile acids make them extremely surface active in lipid digestion.[2] It is known that lipid digestion involves complex interfacial processes, in which bile acids displace conventional surfactants from an emulsified lipid interface to promote the adsorption of lipase to the interface. The adsorbed lipase hydrolyses triglycerides to release fatty acids from the interface. The released fatty acids are then solubilized by bile acid micelles for body adsorption.

Several experimental methods including surface tension,[3,4] zeta potential,[5] atomic force microscopy,[6] and sum frequency generation vibrational spectroscopy[7] have been used to study the interaction of bile acids with conventional surfactants at the oil–water and air–water interfaces to verify the interaction mechanism between bile acids and surfactants in the interfacial process of lipid digestion. Furthermore, the detailed understanding of the interaction of bile acids with surfactants at interfaces can also provide insight into how to control lipid digestion,[8,9] which is critical to prevent the development of obesity and associated diseases.

Liquid crystals (LCs) are an anisotropic fluid, which has a long-range orientational order.[10] The orientation of LCs is extraordinarily sensitive to the change of the surface which they are in contact with. The surface-induced local order can be amplified over several tens of micrometers in the LC bulk due to the long-range interaction of LCs. The optical amplification of LCs makes them a unique optical probe for imaging the molecular ordering[11,12] and chemical patterns[13–15] of organic surfaces and sensing the chemical reactions such as enzymatic reactions,[16,17] DNA hybridization,[18,19] ligand–receptor bindings,[20,21] and peptide–lipid interactions[22,23] at the LC/aqueous interface.

Cholic acid (CA) is a primary bile acid, which comprises 31% of the total bile acids produced in liver. In a previous publication,[24] we used the optical amplification of 4-cyano-4′-pentylbiphenyl (5CB) for studying the competitive adsorption of CA at the surfactant–laden 5CB/aqueous interface. The competitive adsorption of CA can displace the surfactants from the 5CB/aqueous interface and consequently triggers a homeotropic-to-planar anchoring transition of 5CB at the interface, which allows the interaction of CA with the surfactants at the interface to be monitored by a polarizing optical microscope. The concentration of CA required to displace the surfactants from the 5CB/aqueous interface is found to be affected by the nature of surfactants, pH values and ionic strengths. However, the displacement of surfactants from the LC/aqueous interface by the competitive adsorption of CA might be also associated with their interactions with LCs at the interface. To gain insights into the influence of the interaction on the displacement of surfactants from a LC/aqueous interface by the competitive adsorption of CA, we have formed a sodium dodecyl sulfate (SDS)-laden LC/aqueous

[a]*CREOL, The College of Optics and Photonics, University of Central Florida, Orlando, Florida, 32816, USA*

[b]*Department of Materials Science and Engineering, University of Central Florida, Orlando, Florida, 32816, USA. E-mail: jfang@mail.ucf.edu; Fax: +1-407-882-1462; Tel: +1-407-882-1182*

[c]*Material and Chemical Research Laboratories, Industrial Technology Research Institute, Hsinchu, Taiwan. E-mail: swu@creol.ucf.edu; Tel: +1-407-823-4763*

interface with a series of cyanobiphenyl (*n*CB, $n = 5$–8) and the mixture of 5CB with 4-(4-pentylcyclohexyl)benzonitrile (5PCH) or 4-(4-pentylcyclohexyl)cyclohexylcarbonitrile (5CCH) to alter the interaction of SDS and LCs at the interface. We find that the critical concentration of CA required to displace the SDS from the LC/aqueous interface can be linearly tuned by varying the alkyl chain length of *n*CB or the 5PCH concentration in the 5CB host. Significantly, we show that the critical concentration of CA can be reduced by one order of magnitude when the 5PCH concentration increases from 0 wt% to 19 wt% due to the decreased SDS and LC interactions at the interface.

2. Experimental

2.1. Materials

Liquid crystals (LCs) used in our experiments are 4-cyano-4′-pentylbiphenyl (5CB), 4-cyano-4′-hexylbiphenyl (6CB), 4′-heptyl-4-biphenylcarbonitrile (7CB), 4-octyl-4′-cyanobiphenyl (8CB), 4-(4-pentylcyclohexyl)benzonitrile (5PCH), and 4-(4-pentylcyclohexyl)cyclohexylcarbonitrile (5CCH). 5CB (98% purity) and 5PCH (99% purity) were obtained from Sigma-Aldrich (St. Louis, MO). 6CB (98% purity) and 7CB (98% purity) were from BDH Merck Ltd (Poole Dorset, United Kingdom). 5CCH (99% purity) was from EM Industries Inc. (Hawthorne, NY). Sodium dodecyl sulfate (SDS, ≥99% purity) and cholic acid (CA, ≥98% purity) were obtained from Sigma-Aldrich (St. Louis, MO). Cholyl-lysyl-fluorescein (CLF) was purchased from BD Biosciences (Woburn, MA). All chemicals were used without further purification. Water used in our experiments was purified using an Easypure II system (18.2 MU cm and pH 5.7). Phosphate buffered saline solution (PBS) was from Fisher Scientific (Fair Lawn, NJ). Polyimide coated glass substrates used for inducing homeotropic anchoring of liquid crystals were purchased from AWAT PPW (Warsaw, Poland). Glass microscopy slides were from Fisher Scientific. Copper TEM grids (18 μm thickness, 285 μm grid spacing, and 55 μm bar width) were obtained from Electron Microscopy Sciences.

2.2. Preparation of liquid crystal films

Copper TEM grids were cleaned with ethanol and then heated at 110 °C for 24 h. The cleaned TEM grids were placed on a polyimide-coated glass substrate. One microliter of LCs was filled in the pores of the TEM grids supported by the polyimide-coated glass substrate. The excess LC was removed by using a capillary tube, leading to the formation of LC films in the pores of the grids. The LC films were then immersed in PBS solution containing 50 μM SDS. The adsorption of SDS leads to the formation of a SDS-laden LC/aqueous interface.

2.3. Optical observation

The optical texture of the LC films filled in the pores of the TEM grids was examined by using a polarizing optical microscope (BX 40, Olympus) with a hot stage in transmission mode. All optical microscopy images were taken with a digital camera (C2020 Zoom, Olympus) mounted on the polarizing optical microscope. Fluorescence microscopy images were acquired with a confocal fluorescence microscope (Zeiss TCS SP5MP) with 488 nm excitation from an Ar^+ laser.

3. Results and discussion

The chemical structures of CA, SDS, *n*CB ($n = 5$–8), 5PCH, and 5CCH are shown in Fig. 1. SDS is a surfactant with a hydrophilic head group and a long hydrophobic tail. CA is a facial amphiphile molecule with a quasi-planar steroid ring system bearing four hydrogen atoms at the convex face and three hydroxyl groups at the concave face. The phase transition temperatures of *n*CB, 5PCH, and 5CCH are listed in Table 1.

Fig. 2a shows a polarizing optical microscopy image of a 5CB film filled in the square pores of a TEM grid supported by a polyimide-coated glass substrate after being immersed in phosphate buffered saline (PBS) solution with 50 μM SDS. The adsorption of SDS at the 5CB/aqueous interface leads to the formation of the SDS-laden 5CB/aqueous interface and induces homeotropic surface anchoring, giving a dark appearance. The edges of the square pores are lighted up due to the disorder of 5CB near the edges. However, it is clear from Fig. 2a that the edge effect can only extend over a short distance. CA was added into the aqueous phase side of the SDS-laden 5CB/aqueous interface one hour after the system reached equilibrium. The optical appearance of the 5CB film changes from the dark to four-brush textures emanating from a sing line defect (Fig. 2b and c). The appearance of the bright domains reflects a continuous change in the orientation of the 5CB from

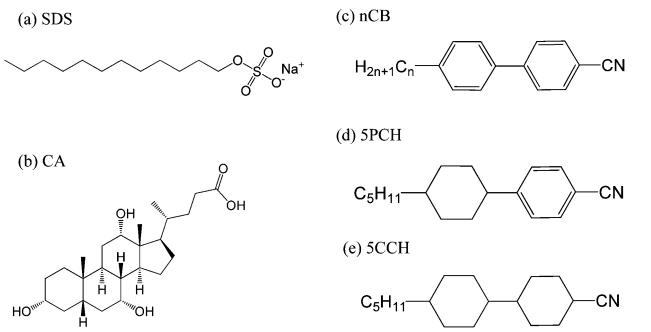

Fig. 1 Chemical structures of SDS (a), CA (b), *n*CB (c), 5PCH (d) and 5CCH (e).

Table 1 Phase transition temperatures of *n*CB, 5PCH and 5CCH. Cr denotes the crystalline phase; S denotes the smectic phase; N denotes the nematic phase; and I denotes the isotropic phase. The phase transition data are obtained from a liquid crystal database Liq46 (LCI Publisher GmbH)

Liquid crystals	Phase transition temperatures (°C)
5CB	Cr 23.5 N 35 I
6CB	Cr 14.5 N 29 I
7CB	Cr 30 N 42.8 I
8CB	Cr 21.5 S 33.5 N 40.5 I
5PCH	Cr 31 N 55 I
5CCH	Cr 60 N 85 I

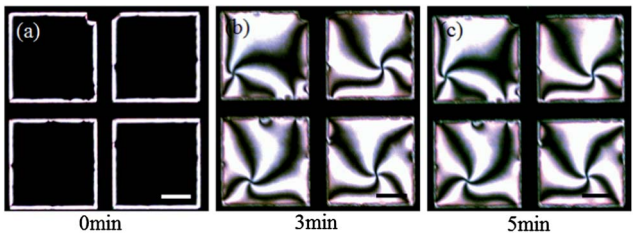

Fig. 2 Polarizing optical microscopy images of a SDS-laden 5CB/aqueous interface after being exposed to 80 μM CA in PBS solution at pH 7.4 and 25 °C. These images were taken at different times. Scale bar: 97 μm.

homeotropic anchoring at the polyimide-coated glass substrate to planar anchoring at the SDS-laden 5CB/aqueous interface.[16] The homeotropic-to-planar anchoring transition of the 5CB at the interface is a result of the competitive adsorption of CA, which displaces the SDS from the interface. Fig. 3a shows a confocal fluorescent microscopy image of the SDS-laden 5CB/aqueous interface after the addition of choly-lysyl-fluorescein (CLF, a fluorescein-labeled CA) into the aqueous phase side of the interface. The strong fluorescence from the interface confirms the competitive adsorption of CLF at the SDS-laden 5CB/aqueous interface. The corresponding polarizing microscopy image shows the bright domain appearance of the 5CB film after the adsorption of CLF at the interface (Fig. 3b). Thus, we conclude that the competitive adsorption of CLF displaces the SDS from the 5CB/aqueous interface, consequently triggering the anchoring transition of the 5CB at the interface. The critical concentration of CLF required to trigger the homeotropic-to-planar surface anchoring transition of the 5CB at the interface is ~0.25 μM, which is lower than that of CA (~16 μM) (Fig. 4). This result suggests that the fluorescent-labeling affects the interaction of CA and SDS at the 5CB/aqueous interface.

We find that the displacement of the SDS at the LC/aqueous interface by the competitive adsorption of CA is strongly affected by the nature of LCs. In our experiments, the SDS-laden LC/aqueous interface was formed with *n*CB, (n = 5–8) and the mixture of 5CB with 5PCH or 5CCH. Since the temperature of the nematic phase of *n*CB varies as a function of n (Table 1), we carried out the experiments at different temperatures to ensure that *n*CB is in their nematic phases. The *n*CB film filled in the

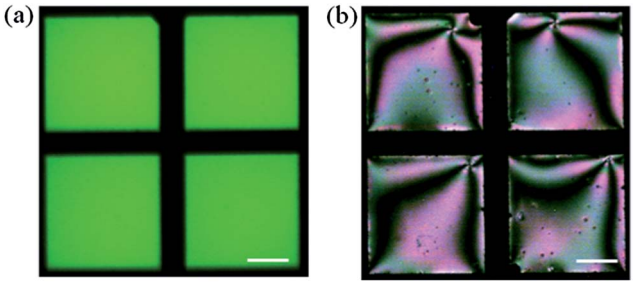

Fig. 3 Fluorescence (a) and polarizing (b) microscopy images of a SDS-laden 5CB/aqueous interface after being exposed to 0.25 μM CLF solution at 25 °C. Scale bar: 97 μm.

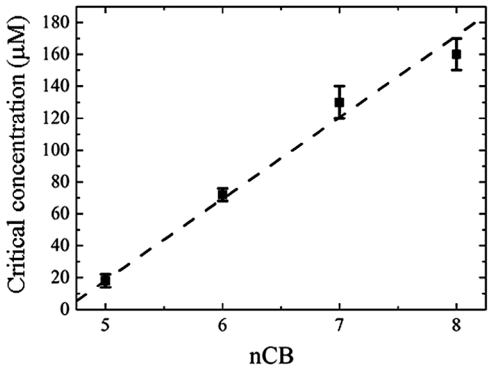

Fig. 4 Critical concentration of CA required for displacing the SDS from the *n*CB/aqueous interface as a function of n. The experiment was conducted at 25 °C for 5CB, 22 °C for 6CB, 32 °C for 7CB, and 36 °C for 8CB, respectively. The data points were obtained from three samples. The error bars represent the standard error.

pores of a TEM grid supported by a polyimide-coated glass substrate was immersed in PBS solution with 50 μM SDS. After the homeotropic anchoring of the *n*CB at the interface was achieved by the adsorption of SDS at the interface, CA was added to the aqueous phase side of the SDS-laden *n*CB/aqueous interface. The critical concentration of CA required to displace the SDS at the *n*CB/aqueous interface is found to linearly decrease from 160 μM to 16 μM as n decreases from 8 to 5 (Fig. 4). Thus, we estimate that the critical concentration decreases by ~51 μM per one additional carbon atom in the alkyl chain of *n*CB. Since the competitive adsorption of CA at the SDS-laden *n*CB/aqueous interface was carried out at different temperatures, we study the possible influence of temperatures on the critical concentration by performing the competitive adsorption at different temperatures in the nematic phase of 6CB and 5CB, respectively. 5CB shows a nematic phase from 23.5 °C to 35 °C. 6CB shows a nematic phase from 14.5 °C to 29 °C. Due to the odd–even effect, the melting and clearing temperatures of 6CB are lower than that 5CB. We find that there is no significant change in the critical concentration observed when temperatures vary from 15 °C to 26 °C for 6CB and 24 °C to 33 °C for 5CB, respectively (Fig. 5). The orientation of LCs is known to be determined by the balance between the elasticity and the surface anchoring. Thus, the changes in the elastic constant of *n*CB and/or the interaction of SDS with *n*CB at the interface are potentially factors that affect the critical concentration. It has been shown that the elastic constant of *n*CB (n = 5–8) alternately changes with the increase of n.[25] The odd–even effect of the elastic constant cannot explain the linear increase of the critical concentration with the increase of n. In the past, orientational wetting studies of *n*CB (n = 5–9) on a surfactant-coated glass substrate showed that the partial-to-complete wetting transition of *n*CB occurred with the increase of n, indicating that the interaction of *n*CB with the surfactant increased with the increase of n.[26,27] Thus, we conclude that the decreased interaction between SDS and *n*CB with the decrease of n makes the SDS more easily displaced from the interface by

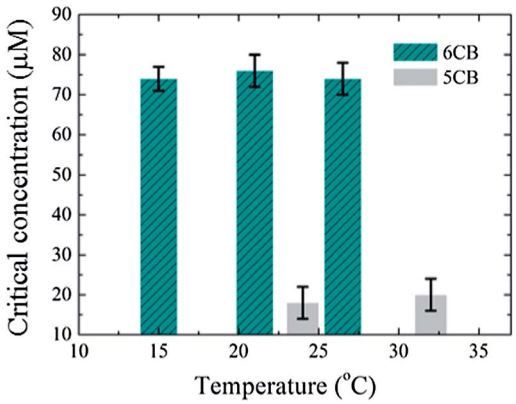

Fig. 5 Critical concentration of CA required for displacing the SDS from the 5CB/aqueous interface and the 6CB/aqueous interface at different temperatures. The data points were obtained from three samples.

the competitive adsorption of CA, leading to the decrease of the critical concentration of CA.

The response time of the SDS-laden *n*CB/aqueous interface for the competitive adsorption of CA varies as a function of *n*. The 5CB undergoes a transition from the dark to four-brush texture within 3 min after addition of 80 μM CA (Fig. 2). While the 6CB transits from the dark to domain textures within 5 min after addition of 80 μM CA. The initially formed domain textures then gradually fuse into the brush textures after 5 hours (Fig. 6), suggesting that the competitive adsorption of CA at the SDS-laden 6CB/aqueous interface follows a nucleation and growth mechanism. For the 7CB and 8CB, the transition from the dark to four-brush texture takes even longer time.

As can be seen in Fig. 4, the critical concentration is 16 μM for 5CB and 130 μM for 7CB, respectively. The critical concentration in this range can be tuned by mixing 7CB and 5CB. The clearing temperature is 35 °C for 5CB and 42.8 °C for 7CB, respectively. Thus, we prepared 7CB–5CB mixtures with different mixed ratios at ~60 °C. The mixtures were then cooled down to ~24 °C, at which the mixtures show a nematic phase. The adsorption of SDS at the 7CB–5CB mixture/aqueous interface induces homeotropic anchoring of the 7CB–5CB mixture at the interface. The displacement of the SDS from the interface by the competitive adsorption of CA leads to the homeotropic-to-planar anchoring transition of the mixture at the interface. The critical concentration of CA is found to linearly decrease from 130 μM to 16 μM when the 7CB–5CB mixed ratio increases (Fig. 7).

5PCH is another widely used cyano-containing LC (Fig. 1). As compared to 5CB, 5PCH has a flexible and bulky core containing one phenyl ring and one cyclohexane ring. We find that the adsorption of SDS at the 5PCH/aqueous interface is unable to induce a homeotropic anchoring of the 5PCH at the interface. As can be seen in Fig. 8a, a tilted anchoring of the 5PCH at the SDS-laden interface is achieved. It has been shown that the tilt angle of the 5CB at the 5CB/aqueous interface can be determined from the interference color of 5CB films filled in the pores of the TEM grids.[28] The thickness of 5PCH films filled in the pores of the TEM grids is ~18 μm. At 25 °C, the extraordinary and ordinary refractive index of 5PCH is 1.60751 and 1.49018, respectively. The effective birefringence of the 5PCH films is estimated to be 0.033 from their optical textures (Fig. 8a) and a Michel-Levy chart.[29] Based on the relationship between the effective birefringence of LC films and the tilt angle of the LC at the LC/aqueous interface,[30] we estimate that the 5PCH is tilted by ~61° from the surface normal (Fig. 8a). The anchoring behavior of 5CB and 5PCH on lecithin monolayers formed by the Langmuir–Blodgett technique was reported in the literature.[31] On densely packed lecithin monolayers, 5CB showed homeotropic anchoring, while 5PCH showed tilted anchoring,

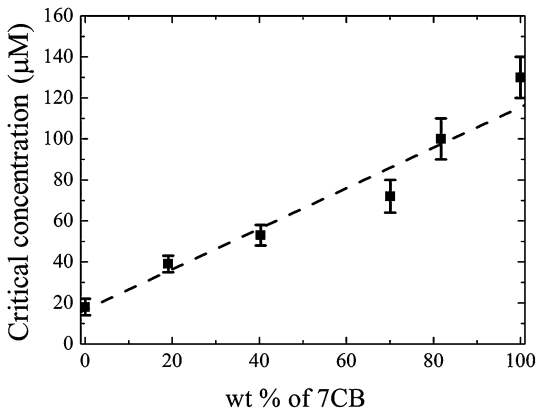

Fig. 7 Critical concentration of CA required for displacing the SDS from the 5CB–7CB mixture/aqueous interface as a function of wt% of 7CB. The data points were obtained from three samples.

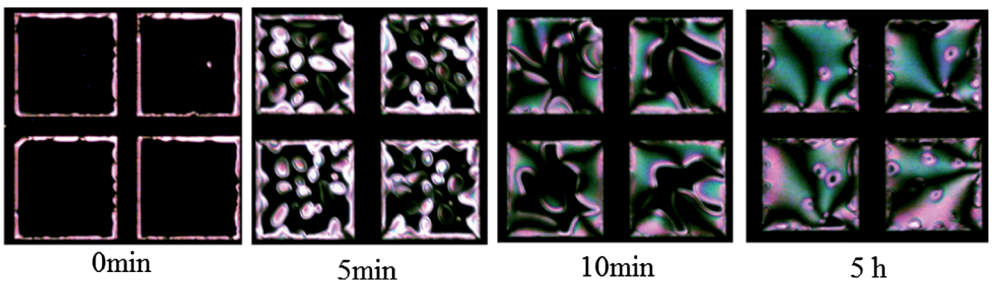

Fig. 6 Polarizing optical microscopy images of the SDS-laden 6CB/aqueous interface after addition of 80 μM CA in PBS solution at pH 7.4 at 25 °C. These images were taken at different times.

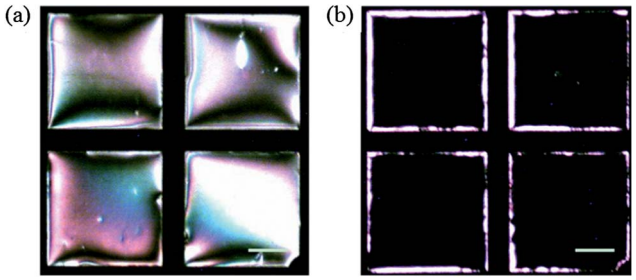

Fig. 8 Polarizing optical microscopy images of a SDS-laden 5PCH/aqueous interface (a) and a SDS-laden 5PCH–5CB mixture/aqueous interface (b). The wt% of 5PCH in the mixture is 17 wt%. Scale bar: 97 μm.

which agrees with our results. The flexible and bulky 5PCH requires higher anchoring energy to achieve homeotropic anchoring than rigid 5CB. It has been shown that 5PCH and 5CB can form nematic mixtures over a wide range of mixed ratios.[32] We prepared 5PCH–5CB mixtures with different mixed ratios at ~70 °C. The mixtures were then cooled down to ~24 °C, at which the mixtures show a nematic phase. The adsorption of SDS at the 5PCH–5CB mixture/aqueous interface can induce a homeotropic anchoring of the 5PCH–5CB mixtures with the mixed ratio up to 19 wt% of 5PCH (Fig. 8b). Beyond this mixed ratio, SDS is unable to induce a homeotropic anchoring of the 5PCH–5CB mixtures at the interface. Thus, we formed the SDS-laden 5PCH–5CB mixture/aqueous interface by using the 5PCH–5CB mixtures with the mixed ratios from 0 wt% to 19 wt% of 5PCH. The critical concentration of CA is found to linearly decrease from 16 μM to 1.5 μM when the mixed ratio increases from 0 wt% to 19 wt% of 5PCH (Fig. 9a). It has been shown that the strong coupling of 5CB molecules is due to the large π–π interaction of their rigid cores (biphenyl rings), while 5PCH molecules are weakly coupled due to the presence of a bulky cyclohexane ring in their core structures.[33] Thus, the looser molecular packing of 5PCH–5CB mixtures makes the SDS more easily to be displaced from the interface by the competitive adsorption of CA, leading to the decrease of the critical concentration of CA.

As shown in Fig. 1, 5CCH contains two bulky cyclohexane rings in its core. The 5CCH–5CB mixture with different mixed ratios was prepared at ~90 °C and then cooled down to ~24 °C. The adsorption of SDS at the 5CCH–5CB mixture/aqueous interface induced a homeotropic anchoring of the 5CCH–5CB mixture with the mixed ratio up to 16 wt% of 5CCH. The critical concentration of CA required to displace the SDS from the 5CCH–5CB mixture/aqueous interface linearly decreases from 16 μM to 6 μM with the increase of the mixed ratio from 0 wt% to 16 wt% of 5CCH (Fig. 9b). The behavior of 5CCH–5CB mixtures in the detection of the displacement of SDS by the competitive adsorption of CA is similar to that of 5PCH–5CB mixtures, suggesting that an additional cyclohexane ring in the core of 5CCH does not significantly affect the molecular packing in the mixtures.

In summary, we have studied the effect of LC structures on the interaction of SDS and CA at the LC/aqueous interface by observing the anchoring transition of the LC at the interface. We find that the critical concentration of CA required to displace SDS from the LC/aqueous interface linearly decreases from 160 μM to 16 μM when the alkyl chain length of *n*CB is reduced from $n = 8$ to $n = 5$. By using 5PCH–5CB mixtures, the critical concentration of CA can be further reduced from 16 μM to 1.5 μM when the mixed ratio increases from 0 wt% to 19 wt% of 5PCH. The reduced critical concentration of CA is a result of the decrease of the interaction of SDS with LCs at the interface, which makes SDS more easily displaced from the interface by the competitive adsorption of CA. Our results show that 5PCH–5CB mixtures are more sensitive in monitoring the interaction of CA and SDS at the LC/aqueous interface, compared to 5CB. In addition, the clearing temperature (N–I transition) is 55 °C for 5PCH (Table 1), which is higher than that of 5CB (35 °C). The clearing temperature of 5PCH–5CB mixtures linearly increases with wt% of 5PCH.[32] Thus, the sensitive 5PCH–5CB mixtures can be operated in a wide temperature range to study the interaction between bile acids and surfactants at the LC/aqueous interface.

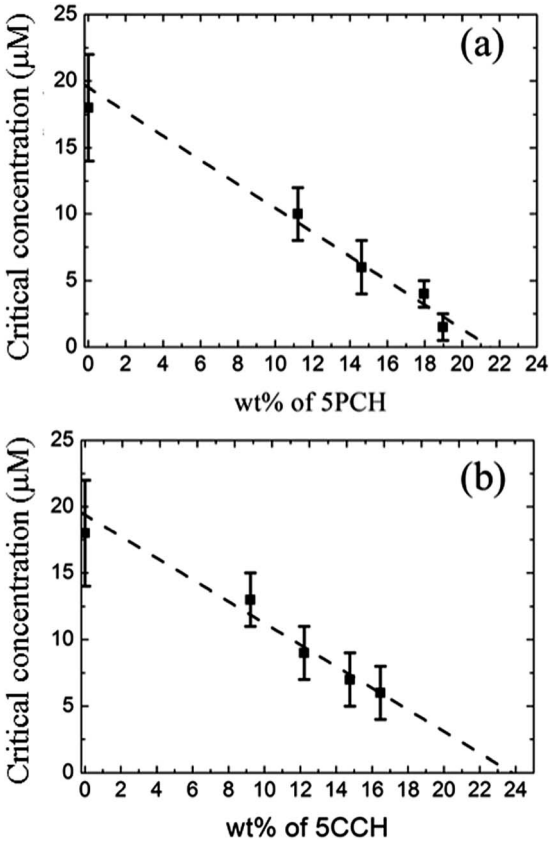

Fig. 9 Critical concentration of CA required for displacing the SDS from the 5PCH–5CB mixture/aqueous interface (a) and the 5CCH–5CB mixture/aqueous interface as a function of wt% of 5PCH and 5CCH, respectively. The data points were obtained from three samples.

Acknowledgements

The authors acknowledge Drs Kevin Belfield and Ciceron Yanez for their assistance with confocal fluorescence microscope. This

work was supported by the Industrial Technology Research Institute (Taiwan) and the US National Science Foundation (CBET-1264355).

References

1 A. F. Hofmann and L. R. Hagey, *Cell. Mol. Life Sci.*, 2008, **65**, 2461–2483.
2 P. J. Wilde and B. S. Chu, *Adv. Colloid Interface Sci.*, 2011, **165**, 14–22.
3 J. M. Kauffman, R. Pellicciari and M. C. Carey, *J. Lipid Res.*, 2005, **46**, 571–581.
4 Z. Vinarov, S. Tcholakova, B. Damyanova, Y. Atanasov, N. D. Denkov, S. D. Stoyanov, E. Pelan and A. Lips, *Langmuir*, 2012, **28**, 12140–12150.
5 A. Torcello-Gómez, J. Maldonado-Valderrama, A. Martín-Rodríguez and D. J. McClements, *Soft Matter*, 2011, **7**, 6167–6177.
6 B. S. Chu, A. P. Gunning, G. T. Rich, M. J. Ridout, R. M. Faulks, M. S. J. Wickham, V. J. Morris and P. J. Wilde, *Langmuir*, 2010, **26**, 9782–9793.
7 P. Ye, Y. J. Xu, Z. P. Han, P. C. Hu, Z. L. Zhao, X. L. Lu and H. G. Ni, *Biochem. Eng. J.*, 2013, **80**, 61–67.
8 H. Singh, A. Ye and D. Horne, *Prog. Lipid Res.*, 2009, **48**, 92–100.
9 B. S. Chu, G. T. Rich, M. J. Ridout, R. M. Faulks, M. S. J. Wickham and P. J. Wilde, *Langmuir*, 2009, **25**, 9352–9360.
10 P. G. De Gennes, *The Physics of Liquid Crystals*, Clarendon, Oxford, 1974.
11 J. Y. Fang, U. Gehlert, R. Shashidar and C. M. Knobler, *Langmuir*, 1999, **15**, 297–299.
12 A. D. Price and D. K. Schwartz, *J. Phys. Chem. B*, 2007, **111**, 1007–1025.
13 V. K. Gupta and N. L. Abbott, *Phys. Rev. E: Stat. Phys., Plasmas, Fluids, Relat. Interdiscip. Top.*, 1996, **54**, R4540–R4543.
14 Y. L. Cheng, D. N. Batchelder, S. D. Evans, J. R. Henderson, J. E. Lydon and S. D. Ogier, *Liq. Cryst.*, 2000, **27**, 1267–1275.
15 T. Bera, W. Liang and J. Y. Fang, *Colloids Surf., A*, 2012, **395**, 32–37.
16 J. M. Brake, M. K. Daschner, Y. Y. Luk and N. L. Abbott, *Science*, 2003, **302**, 2094–2097.
17 X. Bi, D. Hartono and K. L. Yang, *Adv. Funct. Mater.*, 2009, **19**, 3760–3765.
18 A. D. Price and D. K. Schwartz, *J. Am. Chem. Soc.*, 2008, **130**, 8188–8194.
19 S. L. Lai, D. Hartono and K. L. Yang, *Appl. Phys. Lett.*, 2009, **95**, 153702–153704.
20 D. Hartono, C. Xue, K. L. Yang and L. L. Yung, *Adv. Funct. Mater.*, 2009, **19**, 3574–3579.
21 J. M. Seo, W. Khan and S. Y. Park, *Soft Matter*, 2012, **8**, 198–203.
22 Q. Z. Hu and C. H. Jang, *Analyst*, 2012, **137**, 567–570.
23 J. S. Park and N. L. Abbott, *Adv. Mater.*, 2008, **20**, 1185–1190.
24 S. He, W. Liang, C. Tanner, K. L. Cheng, J. Y. Fang and S. T. Wu, *Anal. Methods*, 2013, **5**, 4126–4130.
25 H. Hakemi, E. F. Jagodzinski and D. B. DuPre, *J. Chem. Phys.*, 1983, **78**, 1513–1518.
26 W. Chen, L. J. Martinez-Miranda, H. Hsiung and Y. R. Shen, *Phys. Rev. Lett.*, 1989, **62**, 1860–1863.
27 B. Alkhairalla, H. Allinson, N. Boden, S. D. Evans and J. R. Henderson, *Phys. Rev. E: Stat. Phys., Plasmas, Fluids, Relat. Interdiscip. Top.*, 1999, **59**, 3033–3039.
28 J. M. Brake, A. D. Mezera and N. L. Abbott, *Langmuir*, 2003, **19**, 8629–8637.
29 F. D. Bloss, *An Introduction to the Methods of Optical Crystallograpy*, Holt, Rinehart and Winston, New York, 1961.
30 D. S. Miller, R. J. Carlton, P. C. Mushenheim and N. L. Abbott, *Langmuir*, 2013, **29**, 3154–3169.
31 K. Hiltrop, J. Hasse and H. Stegemeyer, *Ber. Bunsenges. Phys. Chem.*, 1994, **98**, 209–213.
32 I. C. Khoo and S. T. Wu, *Optics and Nonlinear Optics of Liquid Crystals*, World Scientific Publishing Co. Ltd, 1993, p. 14.
33 J. W. Goodby, *Liq. Cryst.*, 2011, **38**, 1363–1387.